Korean J. Chem. Eng., 34(3), 806-813 (2017)
DOI: 10.1007/s11814-016-0305-1

pISSN: 0256-1115
eISSN: 1975-7220

Adsorption and kinetics of elemental mercury vapor on activated carbons impregnated with potassium iodide, hydrogen chloride, and sulfur

Ha-Na Jang*, Seung-Ki Back*, Jin-Ho Sung*, Bup-Mook Jeong***, Youn-Suk Kang**,***, Chul-Kyu Lee**, Jongsoo Jurng****, and Yong-Chil Seo*,†**

*Department of Environmental Engineering, Yonsei University, Wonju 26494, Korea
**R&D Center, J-E Tech Co., Ltd., Seoul 08584, Korea
***Department of Environmental Energy Engineering, Kyonggi University, Suwon 16227, Korea
****Center for Environment, Health and Welfare Research, Korea Institute of Science and Technology, Seoul 02792, Korea
*****Plant Engineering Center, Institute for Advanced Engineering, Yongin 17180, Korea
(*Received 9 May 2016 • accepted 30 October 2016*)

Abstract−Coal combustion emits large amounts of elemental mercury that cannot be captured by air pollution control devices such as flue gas desulfurization because of its insolubility. Therefore, technological advances are necessary for capturing elemental mercury. We conducted various tests on adsorption of elemental mercury using KI-, HCl-, and S-impregnated activated carbons, which were compared with virgin activated carbon. Tests with virgin activated carbon revealed that the optimal adsorption temperature for capturing elemental mercury was 363 K. The adsorption efficiency for elemental mercury was nearly 100% using activated carbon impregnated with 1% and 5% KI and 1%, 5%, and 10% HCl. Through kinetic analyses of the impregnated activated carbons, the optimal equilibrium adsorption capacities of KI-, HCl-, and S-impregnated activated carbons for mercury were determined to be 333.3, 333.3, and 256.4 mg/g, respectively, by using a pseudo second-order kinetic model.

Keywords: Elemental Mercury, Mercury Adsorption, Mercury Kinetic Analysis, Equilibrium Adsorption Capacity, Initial Sorption Rate

INTRODUCTION

Fossil fuel combustion generates various hazardous air pollutants (HAPs) and releases them into the atmosphere. Among the HAPs, mercury is a major anthropogenic emission pollutant. When emitted to the atmosphere, mercury is transported over long distances from the emission sources, and the transportation distance is associated with the residence time of mercury. Mercury is emitted as species of elemental mercury, oxidized mercury, and particulate mercury [1-5]. Depending on the species, the residence time of elemental mercury can exceed one year; elemental mercury can be transported worldwide before being deposited on the ground. Elemental mercury cannot be captured or destroyed after atmospheric release the emission sources; therefore, the effects of mercury on the environment have become a global concern similar to that of greenhouse gases. After releasing to atmosphere, mercury undergoes a series of complex chemical and physical cycles in the atmosphere, on land, and in water. It gradually accumulates in the food-chain process. During these cycles, it potentially causes severe adverse effects in both humans and the environment [1,2]. Coal-fired power plants are considered as major mercury emission sources. In the United States, 158 tons of mercury is emitted annually from anthropogenic sources into the atmosphere, of which approximately 87%, 10%, and 2% are from combustion sources, manufacturing sources, and area sources, respectively [3]. Among those combustion sources, coal-fired power plants contribute the most to mercury emissions [1-3]. In these plants, mercury is volatilized and converted to elemental mercury at high temperatures, and then subsequently converted to oxidized mercury and particulate mercury in various sequential reactions. Mercury exists in flue-gas as elemental mercury, oxidized mercury, and particulate mercury. Mercury emissions can be controlled by using existing air pollution control devices (APCDs), such as particulate matter control device, sulfur dioxide control device, and nitric oxide control device. According to mercury Information Collection Request (ICR), fabric filters (FF) are used in particulate matter control to remove mercury effectively, whereas electrostatic precipitators (ESPs) are not as effective [3-5]. Although mercury is beneficially captured by various configurations of APCDs, a large proportion of elemental mercury is emitted into the atmosphere because it is hard to remove using existing APCDs in the coal-fired power plants. To enhance the capture efficiency of elemental mercury in flue-gas, injection of sorbents into particulate control devices such as ESPs and FFs in coal-fired power plants appears to be a promising technology. Powder activated carbon (PAC) is a widely tested sorbent for mercury removal in pilot and field tests. Numerous adsorption tests have been conducted for enhancing the mercury capture capability. In particular, PAC has exhibited enhanced mercury adsorption efficiencies after being impregnated using various chemicals, such as Cl, Br, I, and Lee et al. studied elemental mercury adsorption by using I and Cl impreg-

†To whom correspondence should be addressed.
E-mail: seoyc@yonsei.ac.kr

nated activated carbon; the adsorption efficiency varied with temperature and chemical loading [6]. Jurng et al. [7] investigated mercury removal capabilities of incineration flue-gas using S impregnated activated carbon and other sorbents such as S impregnated zeolite and wood char; S impregnated carbon showed the highest removal efficiency for elemental and oxidized mercury in flue-gas. Those results indicated that chemical adsorption performance depended on the adsorption materials. Mercury capture efficiency depends on the chemicals impregnated in activated carbon because the surface properties of impregnated activated carbon were varied during mercury capture [8]. There have been numerous researches on mercury adsorption using impregnated activated carbon; however, it has been still uncertain about the difference of elementary mercury removal performance between halogens and sulfur impregnated activated carbons. In particular, these are not evaluated yet using individual kinetic models. In this study, adsorption efficiency tests for elemental mercury vapor were conducted by comparing virgin activated carbon with KI, HCl, and S impregnated activated carbons. To determine the optimal temperature and sorbent loading in the adsorption tests, adsorption tests for virgin activated carbon were conducted under various experimental conditions. Adsorption tests for KI, HCl and S impregnated activated carbons were conducted at various impregnation rate of activated carbon. Moreover, the adsorption kinetics of KI, HCl, and S impregnated activated carbons were investigated using a pseudo second-order kinetic model.

EXPERIMENTAL METHODS

1. Sorbent Preparation

Typical powder activated carbon manufactured by a domestic company was utilized for mercury adsorption tests. Impregnated activated carbon was prepared using 1%, 5%, and 10% of KI, HCl, and CS_2 solutions for the mercury adsorption tests, respectively. 10 g of PAC was stirred in 100 ml of KI, Cl, and CS_2 solutions for 2 h at 75 °C. After stirring for 2 h, the samples were dried for 6 hours at 105 °C in the oven.

2. Sorbent Analysis

The thermal stabilities of the impregnated samples were tested using a thermogravimetric analyzer (TGA 601, LECO Corporation, MI, USA). The total surface area and pore volume were evaluated using the Brunauer Emmett Teller (BET) method, and the average pore diameter was determined by the Barrett Joiner Halenda (BJH) method. Scanning electron microscope (SEM) analysis was performed using a mini-SEM (EM-30, Elim Global, Seong-Nam, Korea).

Table 1. Summary of experimental conditions for elemental mercury adsorption

Item	Test conditions
Reactor diameter	30 mm
Flow rate	1 Nm^3/hr
Pre-heating temperature	363 K
Operating temperature	363 K
Inlet elemental mercury conc.	420 μg/Nm^3
Loading rate of virgin and impregnated PAC	1 g
Impregnated solution	KI, CS_2, HCl
Impregnated ratio	1%, 5%, 10%

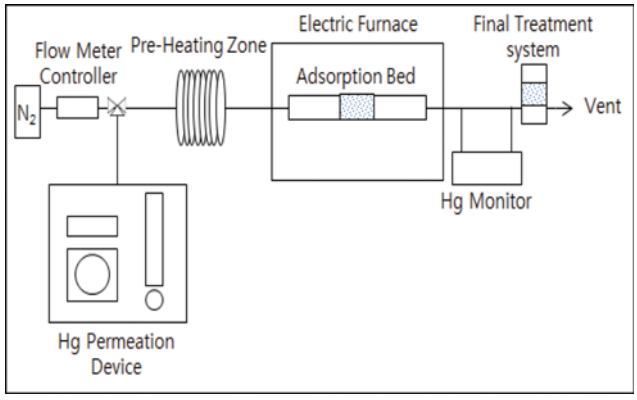

Fig. 1. Schematic diagram of mercury adsorption experimental apparatus.

3. Adsorption Experiment

Table 1 shows a summary of the experimental conditions of adsorption tests in this study. Fig. 1 presents a schematic diagram of the experimental apparatus for mercury adsorption, which consisted of a mercury vapor generation device (Dynacalibrator 230, VICI Metronics, USA), pre-heating zone, fixed-bed type reactor, and mercury continuous emission monitoring (CEM) system (CEM MS-1/DM-5, Nippon Instruments Corporation, Japan). The fixed-bed type reactor was composed of a pre-heater, a simulated gas injection part, an electric furnace, an activated carbon packing column with an 30 mm of inner diameter and 100 mm of length, and a temperature controller. The flow rate of the reactor was 2 Nm^3/hr. The temperature range of the pre-heater was 80-120 °C. The CEM system consisted of the MS-1 speciation unit and two DM-5 detectors. To measure elemental mercury, sample gas and potassium chloride solution were mixed in a reaction tube to remove oxidized mercury. After that, the gas and solution were seperated and elemental mercury was measured. The CEM analyzer was used to directly measure elemental mercury in sample gas on a continuous basis. Oxidized mercury is water-soluble, and it was separated and removed from sample gas by KCl solution. After oxidized mercury in sample gas was eliminated, elemental mercury was measured by CVAA detector.

RESULTS AND DISCUSSION

1. Sorbent Characterization

Table 1 lists the sorbent characteristics of virgin and KI, HCl, and S impregnated activated carbons. As shown in the table, the BET surface area of virgin activated carbon was higher than those of the KI, HCl, and S impregnated activated carbons. The BET surface areas of the impregnated activated carbons tended to decrease as the impregnation ratio increased. In addition, the total pore volume of virgin activated carbon was higher than those of the impregnated activated carbons. A higher impregnation ratio caused in a lower surface area and lower total pore volume, which was not

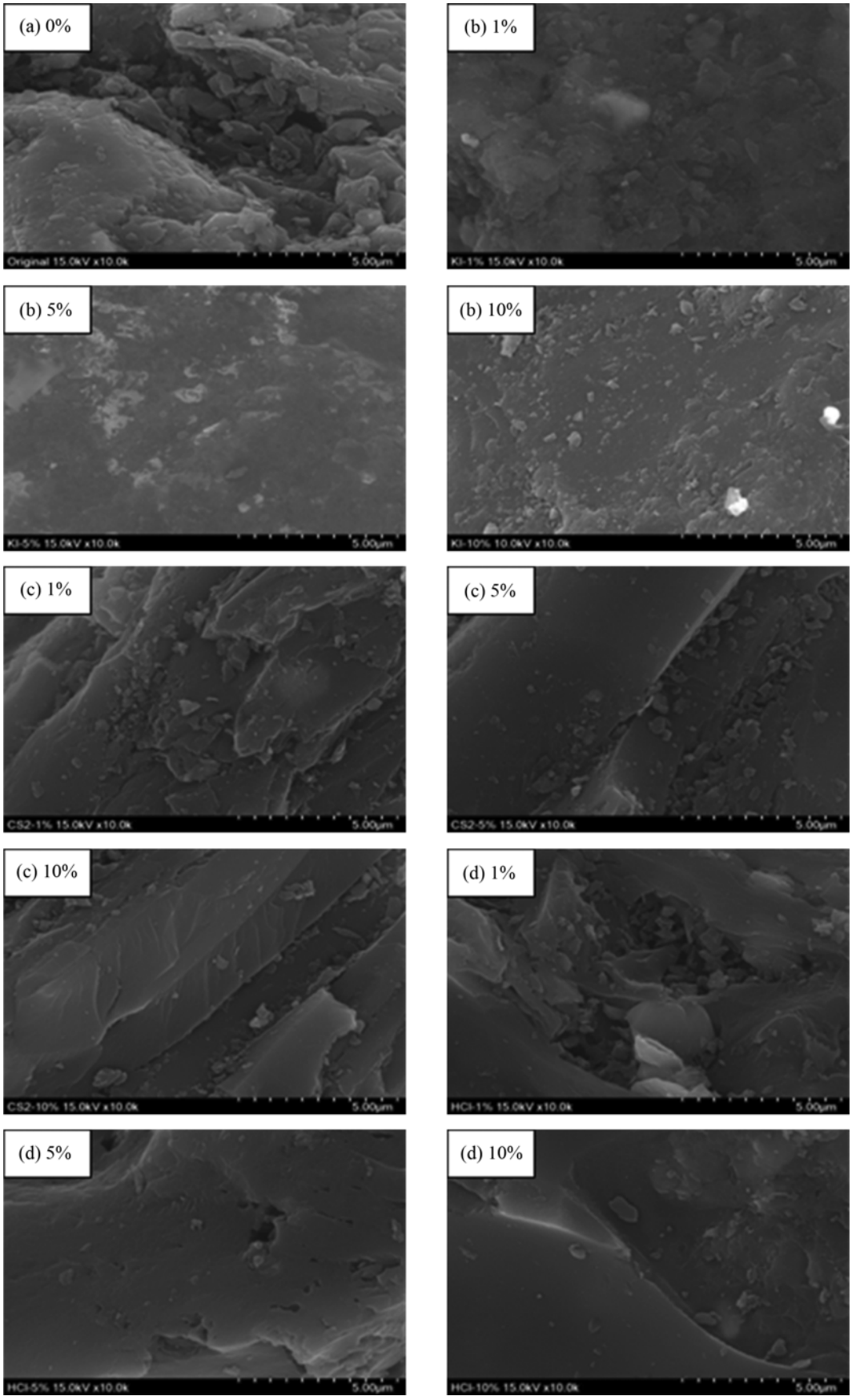

Fig. 2. SEM images of (a) virgin activated carbon and activated carbons impregnated with 1%, 5%, and 10% (b) KI, (c) S, and (d) HCl.

favorable for physical adsorption by activated carbon. It was indicated that chemical adsorption would be more dominant than physical adsorption on the surface of powder activated carbons in case of applying impregnated activated carbon for adsorption tests. Fig. 2 shows SEM pictures of virgin activated carbon and KI-, HCl-, and S impregnated activated carbons. As shown, it was apparent that there was much empty space on the surface of virgin activated carbon, which was porous carbon, for capturing elemental mercury via a physical adsorption mechanism. In the case of impregnated activated carbons, there was not much space on the surface. It indicated that chemical adsorption by impregnated solutions would be more dominant than physical adsorption in capturing elemental mercury on the surface of activated carbons. Fig. 3 shows the thermogravimetric analyzer (TGA) analysis results of activated carbons impregnated using KI, S, and HCl solutions. As shown in those figures, KI- and S-impregnated activated carbons were relatively stable at temperatures higher than 200 °C, which was similar with the typical boiler outlet temperatue in coal-fired power plants. In the case of HCl impregnated activated carbon, the weight loss decreased rapidly at 200 °C; thus, it was relatively unstable in comparison with to KI and S impregnated activated carbons.

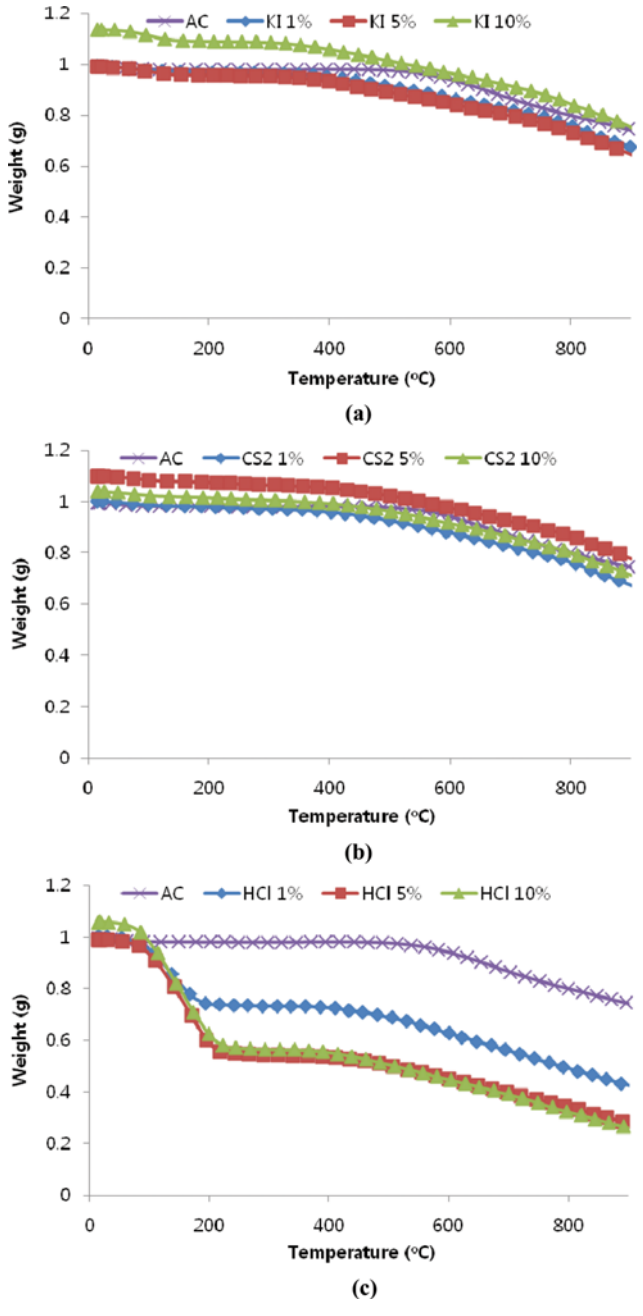

Fig. 3. TGA analysis of activated carbons impregnated with (a) KI, (b) S, and (c) HCl.

2. Adsorption Capability

2-1. Virgin Activated Carbon

Fig. 4(a) shows the mercury adsorption efficiency of virgin activated carbon at different temperatures. The amount of elemental mercury injection for adsorption tests was 420 mg/m^3. Experimental tests for virgin activated carbon were conducted at three temperature cases of 363, 393, and 423 K. To predict adsorption efficiency in high temperature, the loading rate of virgin activated carbon was determined as 3 g. As shown in the figure, the adsorption efficiencies at 393 and 423 K decreased gradually within 1.5 h, respectively. However, the adsorption efficiency at 363 K was maintained at 60-80% within 1.5 h. These results showed that the adsorption temperature affected the mercury capture efficiency of virgin activated carbon. Fig. 4(b) shows the mercury adsorption efficiency with different loadings of virgin-activated carbon. As shown, break-

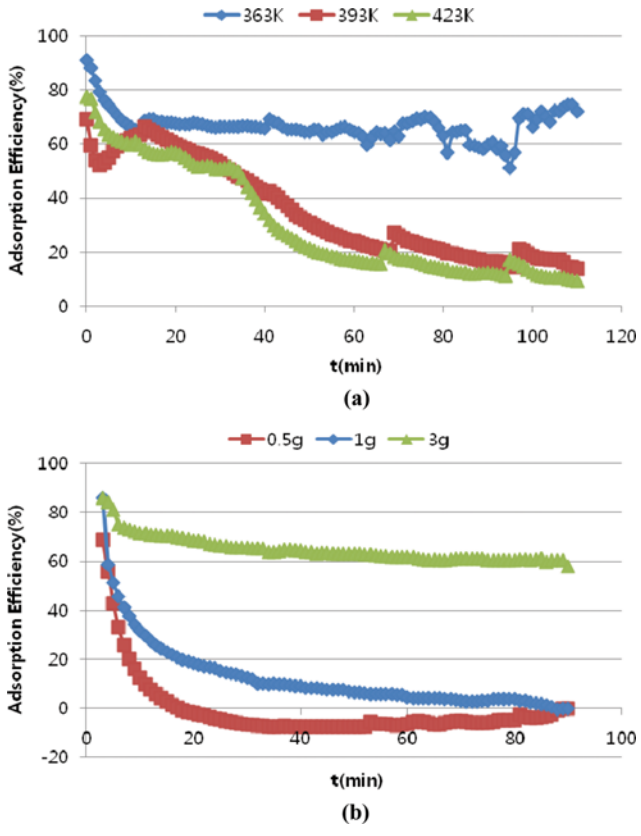

Fig. 4. Mercury adsorption efficiency of virgin activated carbon as a function of time at (a) adsorption temperature, (b) sorbent loading.

through occurred at 20 min with a 0.5 g loading of virgin activated carbon. With a 1 g loading of virgin activated carbon, breakthrough occurred gradually within 1.5 hours. With a 3 g loading, breakthrough did not occur within 1.5 h. Based on those results, 1 g of activated carbon was determined to be the amount used in the impregnated activated carbon experiments, because the difference between virgin activated carbon and activated carbon impregnated using KI, HCl, and S solutions could be clearly observed in later experiments. In addition, the adsorption temperature was determined to be 363 K from the results of the adsorption tests with virgin activated carbon.

2-2. Impregnated Activated Carbons

Fig. 5(a) shows the mercury adsorption efficiency of the impregnated activated carbon with KI solution. As shown, the mercury adsorption efficiency was strongly enhanced by the impregnated activated carbon with KI solution compared with virgin activated carbon. With 1% of KI solution, the adsorption efficiency was maintained at 80-100% within 1.5 hours. With 5% and 10% of KI solution, the adsorption efficiency was maintained at almost 100% within 1.5 hours. Breakthrough did not occur in the cases of 5% and 10% of KI impregnated activated carbon within 1.5 hours. With 1% of KI impinged activated carbon, breakthrough started after 20 minutes, and gradually increased within 1.5 hours. Fig. 5(b) shows the mercury adsorption of the impregnated activated carbon with the S solution. The mercury adsorption efficiency was gradually decreased within 1.5 hours. After 80 minutes, the mercury adsorption efficiency of impregnated activated carbon with 5% and 10% of S solution was decreased to below 40%. With 1% of the CS_2 impinged activated carbon, the breakthrough curve was more slowly increased within 1.5 hours. The mercury adsorption efficiency of 1% of the S impregnated activated carbon was maintained at approximately 80% within 1.5 hours. Fig. 5(c) shows the mercury adsorption efficiency of the impregnated activated carbon with the HCl solution. As shown, the mercury adsorption efficiency of the impregnated activated carbon with 1%, 5%, and 10% of the HCl solution was maintained at almost 100% within 1.5 hours.

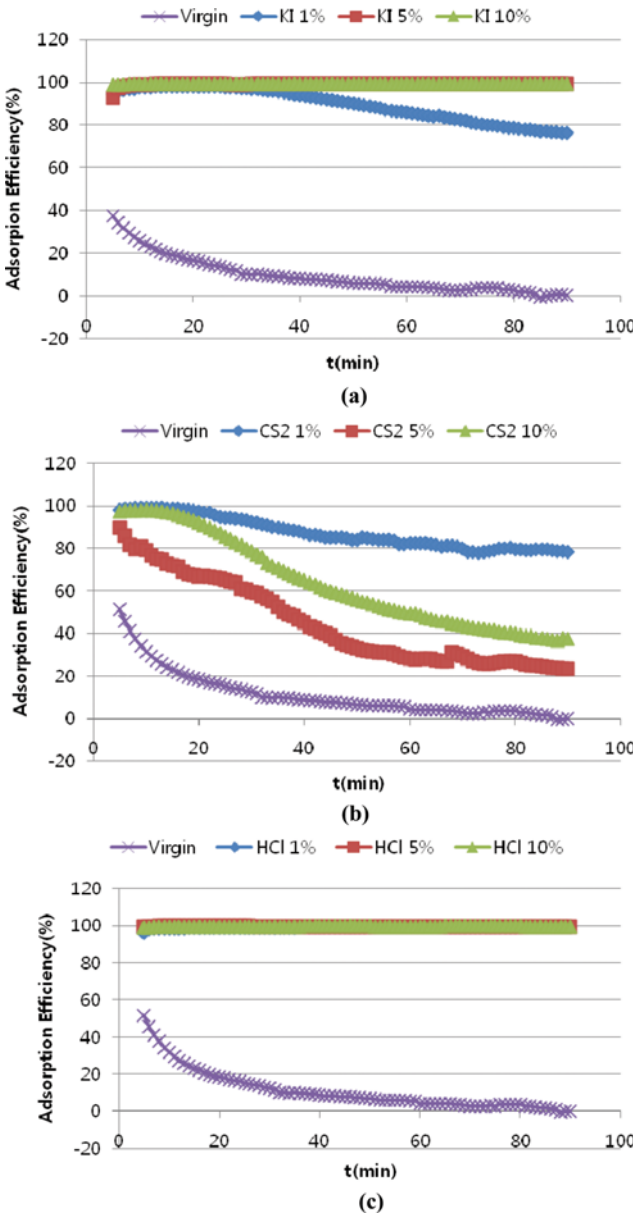

Fig. 5. Mercury adsorption efficiency of impregnated activated carbons (a) KI, (b) S, and (c) HCl.

3. Adsorption Kinetics

During the adsorption process, elemental mercury physically impinged on the sorbent surfaces, and then chemically reacted with the impregnated chemical compounds such as KI, HCl, and S; this is known to be chemisorption. The oxidation and adsorption of elemental mercury can be described by the Deacon process in the following equations [9,10]:

$$Cl_2 \leftrightarrow Cl+Cl \quad (1)$$

$$Hg+Cl \leftrightarrow HgCl \quad (2)$$

$$Hg(g)+Cl_2 \rightarrow HgCl+Cl \quad (3)$$

$$HgCl+Cl_2 \rightarrow HgCl_2+Cl \quad (4)$$

$$HgCl(g) \leftrightarrow HgCl(ads) \quad (5)$$

$$HgCl_2(g) \leftrightarrow HgCl_2(ads) \quad (6)$$

$$HgCl(ads)+Cl \leftrightarrow HgCl_2 \quad (7)$$

The chemical reaction of elemental mercury with KI can be described through the following equations [11,12]:

$$Hg+I_2+2KI \leftrightarrow K_2HgI_4 \quad (8)$$

$$Hg+I_2+2KI \leftrightarrow KHgI_3 \quad (9)$$

$$2KI+HgI+1/2I_2 \leftrightarrow K_2HgI_4 \quad (10)$$

$$KI+HgI+1/2I_2 \leftrightarrow KHgI_3 \quad (11)$$

$$Hg^0+1/2I_2 \leftrightarrow HgI \quad (12)$$

$$Hg^0+I_2 \leftrightarrow HgI_2 \quad (13)$$

The presence of KI influenced favorably the reaction with mercury. Elemental mercury reacted with I_2 and KI on the surface of the impregnated activated carbon. The chemical and physical properties of the S impregnated activated carbon enhance substantially

the capture of elemental mercury [13,14]. To determine the reaction rates of elemental mercury with the KI, HCl, and S impregnated activated carbons, several adsorption kinetic models such as pseudo-first order, pseudo-second order, and Elovich equation were examined to reveal the reaction mechanisms of elemental mercury with those impregnated sorbents. Based on the prediction results, pseudo-first order and Elovich equation model were found to show very low correlation coefficient, and it was confirmed that those models were not able to predict the kinetics on sorption capacity of elemental mercury with impregnated sorbents tested. Among those adsorption kinetic models, the most applicable prediction model was determined as the pseudo-second order model, which could be applied to interpret the chemisorption reaction mechanisms of experimental results. Generally, this model is based on the sorption capacity on the solid phase and has good agreement with chemisorption of impregnated sorbent. When the rate of sorption depends on a second-order mechanism, the pseudo-second order chemisorption kinetic rate equation is expressed as follows [11,15-19]:

$$\frac{dq_t}{dt} = k(q_e - q_t)^2 \tag{14}$$

where q_e and q_t are the sorption capacity at equilibrium and at time t, respectively (μg/g) and k is the rate constant of the pseudo-second order sorption (g/μg·min). The pseudo-second order kinetic parameters q_e and k can be obtained by linearly fitting t/q_t with t. For the boundary conditions t=0 to t=t and q_t=0 to q_t=q_t, the integrated form of the previous equation can be expressed as follows:

$$\frac{1}{(q_e - q_t)} = \frac{1}{q_e} + kt \tag{15}$$

Eq. (15) can be rearranged as follows:

$$q_t = \frac{t}{\frac{1}{kq_e^2} + \frac{t}{q_e}} \tag{16}$$

This can be rewritten in linear form as:

$$\frac{t}{q_t} = \frac{1}{kq_e^2} + \frac{1}{q_e}t \tag{17}$$

where h can be regarded as the initial sorption rate:

$$h = kq_e^2 \tag{18}$$

Table 2 shows the pseudo second-order kinetic parameters of elemental mercury adsorption by KI-, HCl-, and S-impregnated activated carbon. As shown in the table, the R^2 square values ranged from 0.962 to 1. It was indicated that the pseudo second-order kinetics was mostly applicable for the kinetics of those impregnated activated carbons. In the case of KI impregnated activated carbon, the equilibrium sorption capacity, q_e was the highest at 333.3 after using the 5% and 10% KI solutions. The initial sorption rate, h was highest at 1.7×10^4 for the 5% KI impregnated

Table 2. Sorbent characteristics of virgin and KI, S, and HCl impregnated activated carbons

Sorbents	BET surface area (m^2/g)	Total pore volume (cm^3/g)	Average pore diameter (nm)
Virgin	669.3	0.39	3.02
KI 1%	518.0	0.31	2.86
KI 5%	317.9	0.20	3.01
KI 10%	204.4	0.13	3.02
CS_2 1%	664.6	0.39	3.02
CS_2 5%	508.6	0.31	2.90
CS_2 10%	601.6	0.35	3.01
HCl 1%	585.5	0.35	3.01
HCl 5%	544.9	0.32	2.91
HCl 10%	488.5	0.29	3.10

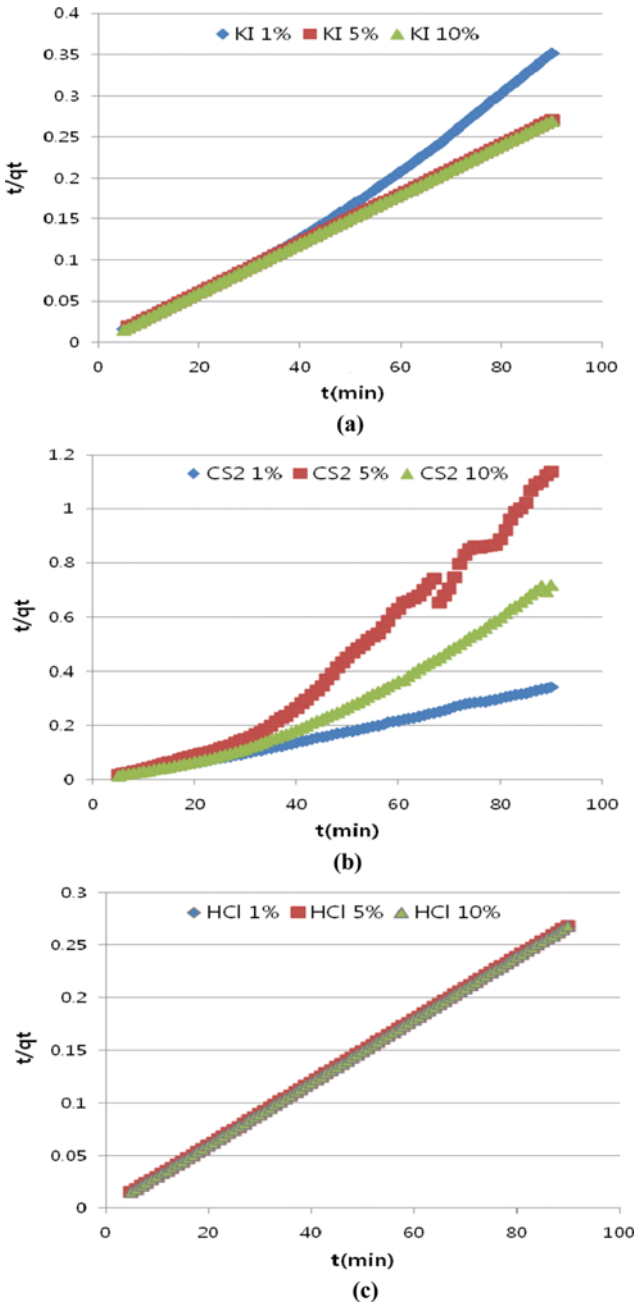

Fig. 6. Pseudo second-order kinetic parameters by the linear method and experimental kinetics of mercury adsorption by impregnated activated carbons (a) KI, (b) S, and (c) HCl.

Table 3. Pseudo second-order kinetic parameters of elemental mercury adsorption by KI, S, and HCl impregnated activated carbons

Sorbents	Pseudo second-order kinetic parameters			
	k (g μg^{-1} min^{-1})	q_e (μg g^{-1})	h=k·q_e^2 (μg g^{-1} min^{-1})	R^2
KI 1%	7.3×10^{-4}	250.0	4.6×10^{1}	0.9914
KI 5%	1.5×10^{-1}	333.3	1.7×10^{4}	1
KI 10%	2.3×10^{-2}	333.3	2.5×10^{3}	1
CS_2 1%	9.3×10^{-4}	256.4	6.1×10^{1}	0.9978
CS_2 5%	9.5×10^{-4}	73.5	0.5×10^{1}	0.9645
CS_2 10%	6.3×10^{-4}	117.6	0.9×10^{1}	0.9620
HCl 1%	2.3×10^{-2}	333.3	2.5×10^{3}	1
HCl 5%	9.0×10^{-2}	333.3	1.0×10^{4}	1
HCl 10%	3.0×10^{-1}	333.3	3.3×10^{4}	1

activated carbon. Fig. 6 shows the pseudo second-order kinetic parameters obtained using the linear method and experimental kinetics of mercury adsorption by KI, HCl, and S impregnated activated carbons. The 5% KI impregnated activated carbon showed the highest mercury adsorption capacity. It did not increase as KI impregnation rate increased. It indicated that an excessive KI impregnation rate could prevent the chemisorption performance on the surface of the impregnated activated carbon. In the case of the S impregnated activated carbon, the R^2 square was not constant in comparison with the KI and HCl impregnated activated carbons. The equilibrium sorption rate was the highest with the 1% S impregnation rate. For HCl impregnated activated carbon, the equilibrium sorption capacity was 333.3 μg/g for all HCl impregnation rates, whereas the initial sorption rate increased as HCl impregnation rate increased. The initial sorption rate of the 10% HCl impregnated activated carbon was the highest among all of the impregnated activated carbons. The various adsorption tests with individual kinetic models revealed that the KI and HCl impregnated activated carbons showed better chemisorption performance for elemental mercury than the S impregnated activated carbon. The halogen solution reacted more with elemental mercury on the surface of activated carbon than sulfuric solution did, and the KI and HCl would be more applicable as impregnation solutions on the surface of activated carbon for the chemisorption of elemental mercury. Based on experimental test results and kinetic model, we concluded that chemisorption mechanism was dominant in halogen impregnated PAC, whereas physical adsorption mechanism was dominant in sulfur impregnated PAC.

CONCLUSIONS

Comparative tests of KI, HCl, and S impregnated activated carbon were conducted to investigate the adsorption performance for elemental mercury. In the TGA tests, the thermal behaviors of KI and S impregnated activated carbons were more stable than that of the HCl impregnated activated carbon. In the tests of virgin activated carbon, sorbent loading and adsorption temperature were determined to be 1 g and 363 K, respectively. In comparison to the virgin activated carbon, the adsorption efficiencies of KI, HCl, and S impregnated activated carbon were strongly enhanced within 1.5 h. In addition, the halogen impregnated activated carbons showed better and more stable performance than the sulfur impregnated activated carbon within 1.5 h. In the pseudo second-order kinetic parameters obtained by the linear method, halogen impregnated activated carbons were more stable than the sulfur impregnated activated carbon, and the equilibrium sorption capacity and initial sorption rate of halogens were higher than those with sulfur. Halogens reacted more with elemental mercury on the surface of activated carbon than sulfur did, and KI and HCl would be more applicable as impregnation solution on the surface of activated carbon for the chemisorption of elemental mercury. However, owing to the thermal instability of HCl impregnated activated carbon, the inlet temperature of sorbent materials should be considered when applied to coal-fired power plants.

ACKNOWLEDGEMENTS

This work is supported by Korea Ministry of Environment as The Eco-Innovation Project. This work is also supported by Korea Ministry of Environment (MOE) as Knowledge-based Environmental Service (Waste to Energy and Recycling) Human Resource Development Project as well.

REFERENCES

1. N. Pirrone and R. Mason, Mercury fate and transport in the global atmosphere (2009).
2. US Environmental Protection Agency, Mercury study report to congress (1997).
3. US Environmental Protection Agency, Control mercury emissions from coal fired electric utility boilers (2005).
4. US Environmental Protection Agency, Preliminary estimates of performance and cost of mercury emission control technology applications on electric utility boilers (2004).
5. J. H. Pavlish, E. A. Sondreal, M. D. Mann, E. S. Olson, K. C. Galbreath, D. L. Laudal and S. A. Benson, *Fuel Processing Technol.*, **82**, 89 (2003).
6. S. J. Lee, Y. C. Seo, J. Jurng and T. G. Lee, *Atmospheric Environ.*, **38**, 4887 (2004).
7. J. Jurng, T. G. Lee, G. W. Lee, S. J. Lee, B. H. Kim and J. Seier, *Chemosphere*, **47**, 907 (2002).
8. A. Saha, *Energy Fuels*, **28**, 4021 (2014).

9. H. Y. Pan, R. G. Minet, S. W. Benson and T. T. Tsotsis, *Ind. Eng. Chem. Res.*, **33**, 2996 (1994).
10. W. Du, L. Yin, Y. Zhuo, Q. Xu, L. Zhang and C. Chen, *Ind. Eng. Chem. Res.*, **53**, 582 (2014).
11. J. Cai, B. Shen, Z. Li, J. Chen and C. He, *Chem. Eng. J.*, **241**, 19 (2014).
12. B. Shen, J. Chen and S. Yue, *Micropor. Mesopor. Mater.*, **203**, 216 (2015).
13. H. C. His, M. J. Rood, M. R. Abadi, S. Chen and R. Chang, *J. Environ. Eng.*, **128**, 1080 (2002).
14. Y. S. Ho and G. McKAY, *Trans Institution Chem. Engineers*, **76**, Part B (1998).
15. K. V. Kumar, *J. Hazard. Mater.*, **137**, 1538 (2006).
16. G. Skodras, I. Diamantopoulou, G. Pantoleontos and G. P. Sakellaropoulos, *Materials*, **158**, 1 (2009).
17. N. Asasian, T. Kaghazchi, A. Faramarzi, A. H-. Siboni, R. A-. Kesheh, M. Kavand and S-. A. *Int. J. Environ. Sci. Technol.*, **45**, 1588 (2014).
18. F. Raji and M. Pakizeh, *Appl. Surf. Sci.*, **301**, 568 (2014).
19. L. Cui, X. Guo, Q. Wei, Y. Wang, L. Gao, L. Yan, T. Yan and B. Du, *J. Colloid Interface Sci.*, **439**, 112 (2015).